Harvesting Kinetic Energy with Switched-Inductor DC–DC Converters

Dongwon Kwon, Gabriel A. Rincón-Mora, and Erick O. Torres
Georgia Tech Analog, Power, and Energy IC Research
{dkwon3, rincon-mora, erick.torres}@gatech.edu

***Abstract*—The potential application space for miniaturized systems like wireless microsensors is expansive, from reconnaissance mission work and remote sensors to biomedical implants and disposable consumer products. Conforming to microscale dimensions, however, constrains energy and power to such an extent that sustaining critical power-hungry functions like wireless communication is next to impossible. Harvesting ambient energy offers an appealing alternative, except the act of transferring energy requires power that could easily exceed what the transducer generates in the first place. This paper presents how to design low-power switched-inductor converters capable of producing net energy gains when supplied from low-power piezoelectric and electrostatic kinetic-harvesting sources.**

I. Harvesting Kinetic Energy in Vibrations

Wireless microsensors can enjoy popularity in, for example, medical treatment [1] and monitoring tire pressure [2] because they offer *in-situ*, real-time, non-intrusive processing capabilities, in other words, because they add intelligence in little to negligible space. The problem is a miniaturized platform necessarily constrains the energy capacity (i.e., operational life) of an on-board battery to impractical levels [3]. Energy harvesting is therefore an attractive alternative, as it continuously replenishes a battery from ambient energy in light, temperature, and/or motion. Of these, solar light produces the highest output power density, except when supplied from indoor lighting under which conditions power decreases drastically [4]. Harnessing thermal energy is viable [5], but microscale dimensions severely limit temperature gradients, the fundamental source from which the device draws energy [3]. Harvesting the kinetic energy in motion may not compete with solar power but, in contrast to indoor lighting and thermal sources, moderate and consistent output power across a vast range of applications is typical [3]–[4].

Although the application ultimately determines which kinetic energy harvesting scheme is optimal, piezoelectric transducers, harvester circuits for which Section II describes, are relatively mature and produce comparatively higher power. On-chip piezoelectric devices, however, are far from mature, which is where electrostatic harvesters (discussed in Section III) find an edge, because microelectromechanical systems (MEMS) technologies can more aptly integrate variable, parallel-plate capacitors on chip [3]–[4]. Magnetic schemes, unfortunately, suffer from low output voltages [3], which practical circuits cannot easily accommodate without sacrificing some, if not all, the energy harvested.

II. Piezoelectric Harvesters

When a mechanical vibration stimulates a piezoelectric material, the internal charge configuration changes to generate a voltage across the surfaces [3]–[4]; in other words, an ac current charges and discharges the capacitance between the surfaces [6]. The purpose of a piezoelectric harvester is to transfer the energy in the form of charge to an intermediate reservoir, such as a capacitor or battery. The harvester does not supply the load directly because the mechanical input is unpredictable and therefore unreliable for on-demand loading events [7]. Considering its aim, the system must therefore condition and rectify an ac source into a dc output without losing considerable energy, which is why efficient rectifiers [8]-[10] and rectifiers with the conditioned input and output voltages that produce higher power [6], [11]–[12] are the subject of ongoing research.

A. Rectifier-Free, Switched-Inductor System

While the efficiency of rectifiers can be high, the power they draw is not because the rectifier only transfers energy when the input voltage exceeds its output. In other words, the rectifier can only harvest for a fraction of the vibration cycle, when the piezoelectric cantilever bends enough to generate a voltage that surpasses the rectified output. To circumvent this fundamental limitation, the harvester, as shown in Fig. 1 [7], [13], can temporarily store the transduced energy in an inductor before delivering it to the storage capacitor or battery.

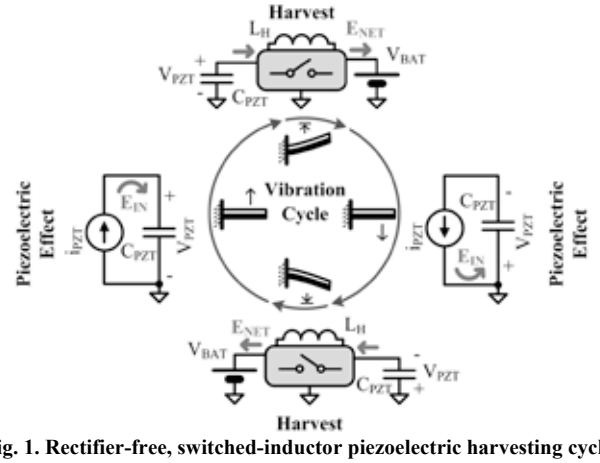

Fig. 1. Rectifier-free, switched-inductor piezoelectric harvesting cycle.

The rectifier-free, switched-inductor harvester in Fig. 1 first allows the half of the vibration to induce the transducer to source current i_{PZT} into piezoelectric capacitance C_{PZT}. Once C_{PZT}'s voltage reaches its peak, which corresponds to the transducer's maximum displacement point, the system transfers C_{PZT}'s stored energy into harvesting inductor L_H, after which point the circuit reconfigures its switches to de-energize L_H into the battery. Because energizing and delivering L_H's energy to the battery only requires a few µs and the vibration period is on the order of ms, the position of

This research is supported by Linear Technology Corporation, Milpitas, CA, and Texas Instruments, Dallas, TX.

the cantilever practically remains unchanged through this L_H's entire energy-transfer process. Similarly, after the other half of the vibration cycle induces the transducer to maximally charge C_{PZT} in the other direction, the harvester discharges C_{PZT} into L_H and then redirects L_H's energy into the battery.

C_{PZT} stores the electrical energy produced by the piezoelectric effect each half cycle, so input energy per cycle E_{IN} is

$$E_{IN} = \tfrac{1}{2}C_{PZT}V_{PZT(PEAK+)}^2 + \tfrac{1}{2}C_{PZT}V_{PZT(PEAK-)}^2, \quad (1)$$

where $v_{PZT(PEAK+)}$ and $v_{PZT(PEAK-)}$ are C_{PZT}'s positive and negative peak voltages, respectively. Without the harvester, the quarter of the vibration cycle after the positive and negative peak points would be used to discharge C_{PZT} from their respective peaks. In contrast, since the harvester extracts all the stored energy in C_{PZT} and resets the voltage to zero at the peaks, the whole vibration cycle is exploited to generate the higher peak voltages compared to the open-circuited counterparts, the maximum input voltage a rectifier-based system can experience. Higher peak voltages thus indicate the harvester draws more energy from the environment.

The driving force behind adopting a switched-inductor topology is L_H and its accompanying switches, which conduct with close to zero voltages across them, dissipate little power. Unfortunately, harvested power can also be low, so parasitic energy losses E_{LOSSES} in L_H's equivalent series resistance (ESR), the switches' turn-on resistances, driving parasitic capacitances of switches, and controller quiescent current I_Q can use a considerable fraction of the energy harvested:

$$E_{LOSSES} = R_{EQ+}I_{L(PEAK+)}^2T_{C+} + R_{EQ-}I_{L(PEAK-)}^2T_{C-} + C_{EQ}V_{BAT}^2 + I_QV_{BAT}T_{VIB}, \quad (2)$$

where $R_{EQ+/-}$ represent the equivalent resistances that conduct peak inductor current $I_{L(PEAK+/-)}$ during conduction time $T_{C+/-}$ for positive and negative half cycles, and C_{EQ} is the total equivalent parasitic capacitance present that must be charged to and discharged from battery voltage V_{BAT} during the vibration period T_{VIB} [7]. Thus, the net energy harvested E_{NET} is necessarily below the energy the transducer avails (E_{IN}):

$$E_{NET} = E_{IN} - E_{LOSSES}. \quad (3)$$

B. Circuit Embodiment

In the circuit shown in Fig. 2, for example, after i_{PZT} charges C_{PZT} across half the vibration cycle to its positive peak voltage, switches S_I and S_N first energize L_H, and S_I and diode-switch D_N then steer L_H's current i_L into V_{BAT}. Similarly, after i_{PZT}'s negative phase charges C_{PZT} to its negative peak voltage, S_I and S_N again energize L_H but now S_N and D_I channel i_L into V_{BAT}. Notice asynchronous diodes D_N and D_I stop conducting when the system depletes L_H: when i_L attempts to reverse.

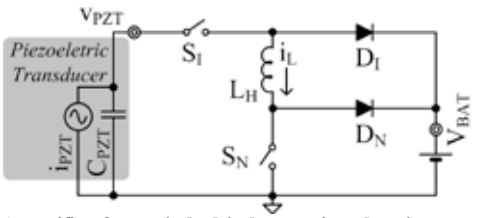

Fig. 2. A rectifier-free switched-inductor piezoelectric power stage.

Since L_H energizes as soon as its terminal voltages surpass zero Volts, the converter avoids the input threshold voltage normally imposed by rectifier-based systems, whose piezoelectric input voltages must exceed their rectified outputs. Additionally, by inverting L_H's output conduction path (between D_N and D_I), the system harnesses energy during the positive and negative vibration cycle, effectively "full-wave rectifying" the ac input without a rectifier circuit.

From a time-domain perspective, piezoelectric voltage v_{PZT} rises (as C_{PZT} charges) through the positive half cycle, as Fig. 3a illustrates from approximately 10.7 to 15.7 ms. When v_{PZT} peaks at 15.7 ms, S_I-L_H-S_N discharge C_{PZT} to ground abruptly. During this quick discharge, S_I-S_N first energizes L_H in 10 µs, as Fig. 3b shows, and S_I-D_N then depletes L_H into V_{BAT} in 1 µs. Similarly, v_{PZT} falls in the negative half cycle from 15.7 to 20.7 ms and S_I-S_N energizes L_H in 10 µs and S_N-D_I drains L_H in 1 µs. The fact L_H de-energizes means i_L flows into V_{BAT}, which is to say the harvester harnesses energy, as the gray rising staircase energy trace E_{NET} in Fig. 3a corroborates.

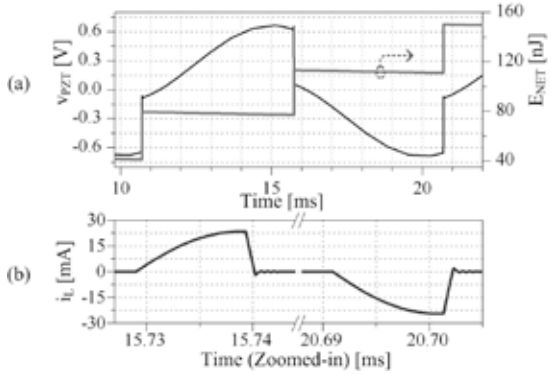

Fig. 3. Simulated waveforms of the piezoelectric harvester.

C. Synchronization and Control

For the system to harvest, it must drain C_{PZT}'s energy into L_H when vibrations maximally charge C_{PZT}. Comparator CP_{PK} in Fig. 4 therefore detects when v_{PZT} peaks by comparing v_{PZT} to its delayed counterpart v_D. Since v_{PZT} leads v_D, the moment v_{PZT} falls below v_D (and CP_{PK} trips) indicates v_{PZT} reached its positive peak. Similarly, v_{PZT} rising above v_D implies v_{PZT} just reached its negative peak. Although CP_{PK} functions continuously, its low bandwidth requirement allows it to operate in subthreshold (with low power).

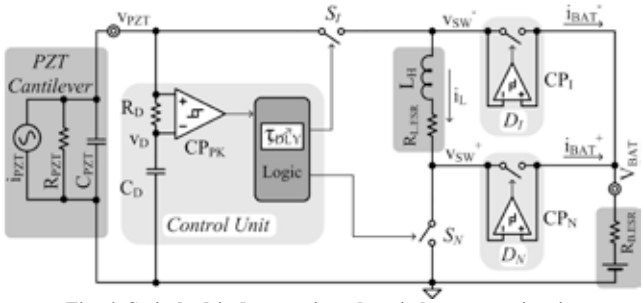

Fig. 4. Switched-inductor piezoelectric harvester circuit.

The system must also detect when to stop energizing L_H. To this end, because C_{PZT} transfers energy to L_H in a quarter of its resonance period, the controller estimates L_H's energizing time by tuning adjustable delay τ_{DLY} in Fig. 4 to $\sqrt{C_{PZT}L_H}$. Note comparator-controlled switches D_I and D_N implement diodes by conducting current i_{BAT} into V_{BAT} only when switching signals v_{SW}^+ and v_{SW}^- surpass V_{BAT}. The power a conventional diode would otherwise dissipate can exceed the

conduction loss across a MOS switch plus the quiescent power through its controlling comparator, which the system only powers on demand, when v_{SW}^+ and v_{SW}^- surpass V_{BAT}.

III. Electrostatic Harvesters

A motion-sensitive, parallel-plate variable capacitor (C_{VAR}) draws kinetic ambient energy by dampening vibration forces [3]. More specifically, as motion separates C_{VAR}'s plates, capacitance decreases and either C_{VAR}'s voltage v_C increases (because q_C equals $C_{VAR}v_C$) to increase its stored energy E_C to $C_{VAR}(v_{Final}^2-v_{Initial}^2)$ or charge q_C decreases (i.e., C_{VAR} releases q_C) to generate current i_{HARV} as $\Delta q_C/dt$. The challenge with keeping q_C constant to augment E_C is that v_C can reach levels (e.g., 100 – 300 V) well above the breakdown voltages of high-volume, low-cost semiconductor technologies (e.g., 5 V). Although constraining voltage harvests less energy (at a linear rate, as opposed to the parabolic rise E_C enjoys in the former case), Δq_C generates power in the more benign form of current:

$$P_C = V_{CONST} i_{HARV} = V_{CONST}\frac{dq_C}{dt} = V_{CONST}\frac{d(C_{VAR}v_C)}{dt} = V_{CONST}^2\frac{dC_{VAR}}{dt}. \quad (4)$$

A. Battery-Constrained and -Directed System

Constraining v_C to a system-generated or intermediate source is possible [14] but fixing v_C to V_{BAT} by connecting C_{VAR} to V_{BAT} is more efficient because C_{VAR} channels i_{HARV} directly into V_{BAT} [15]–[16]. Since C_{VAR} generates q_C when C_{VAR} decreases, the system must first precharge C_{VAR} to V_{BAT} when C_{VAR} peaks at C_{MAX}, as Fig. 5 illustrates. Energizing C_{VAR}, however, represents an energy investment E_{INV} from V_{BAT}:

$$E_{INV} = \tfrac{1}{2}C_{MAX}V_{BAT}^2. \quad (5)$$

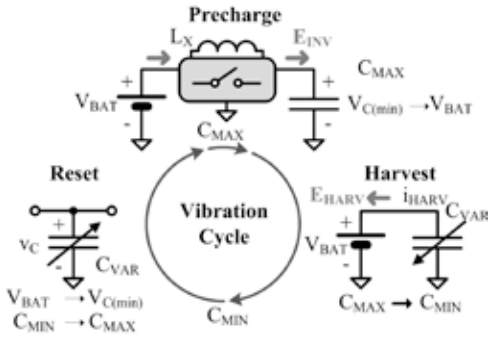

Fig. 5. Battery-constrained and -directed electrostatic harvesting cycle.

The energy harvested E_{HARV} when subsequently connecting C_{VAR} to V_{BAT} and vibrations decrease C_{VAR} to minimum C_{MIN} must exceed E_{INV} and whatever other losses E_{LOSSES} exist for the system to produce a net gain E_{NET}:

$$E_{HARV} = \int V_{BAT} i_{HARV}(t)dt = \Delta C_{VAR} V_{BAT}^2 \quad (6)$$

and

$$E_{NET} = E_{HARV} - E_{INV} - E_{LOSSES} = (0.5C_{MAX} - C_{MIN})V_{BAT}^2 - E_{LOSSES}, \quad (7)$$

where ΔC_{VAR} is $C_{MAX} - C_{MIN}$. To harvest in the next vibration cycle, the system must detach C_{VAR} from V_{BAT} at C_{MIN} (to avoid reverse current from otherwise discharging V_{BAT}) and wait for vibrations to pull C_{VAR}'s plates together until C_{VAR} peaks at C_{MAX}, prompting the system to repeat the sequence.

B. Switched-Inductor Circuit Embodiment

Before attaching C_{VAR} to V_{BAT}, the system must precharge C_{VAR} to V_{BAT} with little to negligible losses, because charging C_{VAR} directly from V_{BAT} through a switch dissipates considerable power with respect to the little energy C_{VAR} induces. As in the piezoelectric case, the switched-inductor harvester in Fig. 6 dissipates little power because energy-transfer inductor L_X and the switches, which conduct with close to zero Volts across them, are nearly lossless. Functionally, S_E energizes L_X from V_{BAT} before disengaging and allowing S_D to deplete L_X into C_{VAR}. Note this precharge phase only lasts a small fraction of the vibration cycle so C_{VAR} remains virtually constant at around C_{MAX} through this phase.

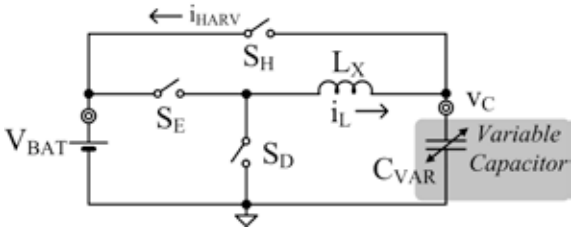

Fig. 6. A switched-inductor, voltage-constrained electrostatic power stage.

After precharging C_{VAR}, the system disengages S_D and connects C_{VAR} to V_{BAT} with S_H to start the harvesting phase. Therefore, as vibrations decrease C_{VAR} from 391 pF to 100 pF, for example, as Fig. 7 shows between 23.7 and 24.05 ms, i_{HARV} flows into a 3.5-V battery. The energy the battery accumulates in one cycle is sufficiently high to overcome its initial investment E_{INV} (-2.75nJ in Fig. 7) and the system's parasitic losses E_{LOSSES} with a net gain, in this case, of 1 nJ per cycle.

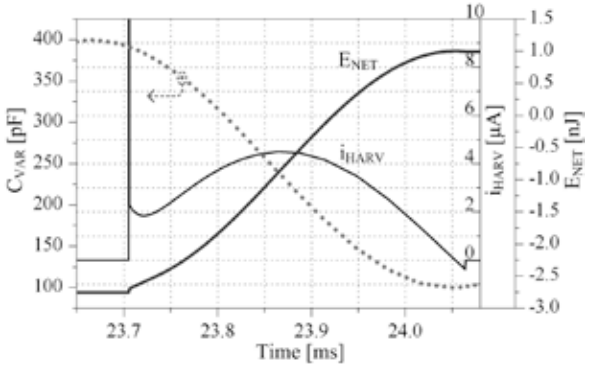

Fig. 7. Simulated waveforms of the electrostatic harvester during the harvesting phase.

C. Synchronization and Control

Notice the harvester must monitor C_{VAR} to precharge and subsequently connect it to V_{BAT} at C_{MAX}. Fortunately, in the reset phase, because C_{VAR} floats when it rises to C_{MAX} and its voltage v_C therefore decreases proportionately (since Q_{CONST} is $C_{VAR}v_C$), sensing when v_C reaches its minimum voltage indicates when C_{VAR} peaks. To this end, as in the piezoelectric case, comparator $CP_{P\text{-}STRT}$ in Fig. 8 senses when v_C, which leads its delayed counterpart v_D, begins to rise above v_D, prompting the logic to start the precharge phase.

Similar to the piezoelectric case, the system must also determine how long to energize L_X to precharge C_{VAR} to V_{BAT}. Consider that undercharging C_{VAR} means S_H will first charge C_{VAR} to V_{BAT} inefficiently at the beginning of the harvesting phase, decreasing the net energy gain of the system. Unfortunately, overcharging C_{VAR} likewise represents a loss

because S_H discharges C_{VAR} to V_{BAT} inefficiently, again, at the beginning of the harvesting phase. Hence, the harvester must tune L_X's energizing time to precisely precharge v_C to V_{BAT} by adjusting delay τ_{DLY} in Fig. 8. Afterwards, $CP_{P\text{-}END}$ detects the end of precharging when L_X depletes (i.e., i_L=0) by comparing the switching node voltage v_{SW} to 0 V, and prompt the harvesting phase to begin by setting S_H's S-R latch.

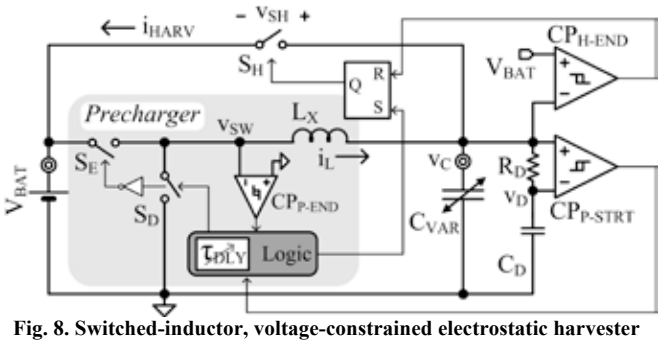

Fig. 8. Switched-inductor, voltage-constrained electrostatic harvester circuit.

In the harvesting phase, i_{HARV} induces a voltage drop across S_H's turn-on resistance that raises v_C slightly above V_{BAT} (by v_{SH}), keeping $CP_{H\text{-}END}$'s output from resetting S_H's S-R latch. Once C_{VAR} reaches C_{MIN} and i_{HARV} consequently falls to zero, v_C drops to V_{BAT} and $CP_{H\text{-}END}$ trips, resetting the latch and disengaging S_H, all of which marks the end of the harvesting phase. Note $CP_{P\text{-}STRT}$, $CP_{P\text{-}END}$, and $CP_{H\text{-}END}$ only operate during their respective phases to conserve energy. Additionally, because the vibration frequency is typically low, the vibration sensing comparators $CP_{P\text{-}STRT}$ and $CP_{H\text{-}END}$ have low bandwidth requirements and are allowed to function properly in subthreshold, with nA's of current.

IV. Discussion

Although the switched-inductor circuits of Figs. 4 and 8 illustrate practical piezoelectric and voltage-constrained electrostatic harvesters, they do not represent all possible embodiments of the same. Manually tuning the energizing time of the inductor, for instance, is not the only means of determining when to stop energizing. A correcting loop that adjusts the delay from cycle to cycle and operates only a fraction of each cycle could also adjust the time, albeit at the cost of additional power losses. Perhaps a more fundamental point to highlight is the significance of producing a net energy gain with these harvesters, even if only a few nJ per cycle. The truth is the power these harvesters generate when constrained to miniaturized platforms is not sufficient to power practical applications like wireless microsensors. Generating power, however, is not as important as accumulating energy because sensors, for the most part, need not operate continuously. In other words, intermediate batteries can supply the power that sensors momentarily require when charged (over time) by these harvesters.

V. Conclusions

The fundamental challenge in harvesting ambient energy with microscale devices is producing a net energy gain, that is to say, conditioning and transferring energy and synchronizing the system to vibrations without dissipating considerable power in the process. Reducing losses is the driving force behind the adoption of switched-inductor circuits, because inductors and switches that conduct while dropping nearly zero Volts are quasi-lossless. One problem is inductors are bulky and difficult to integrate, which is why using only one inductor is so important. Still, small-scale transducers generate little power, losing a considerable portion to otherwise negligible conduction, switching, and quiescent losses and achieving efficiencies of 40-70%, even if functional blocks operate only a fraction of the vibration period with nA's of current [7], [13]. Nevertheless, continuously producing a net output power of even a few μW's can charge a battery so that, when a sensor needs energy, which does not typically happen often, the battery can readily supply it. The idea is to supplement the system with enough energy over time to extend its operational life and avoid having to replace an otherwise easily exhaustible battery.

References

[1] D.A. La Van, T. McGuire, and R. Langer, "Small-scale systems for in vivo drug delivery," *Nature Biotechnology*, vol. 21, no. 10, pp. 1184–1191, Oct. 2003.

[2] M.D. Seeman, S.R. Sanders, and J.M. Rabaey, "An ultra-low-power power management IC for energy-scavenged wireless sensor nodes," *IEEE Power Electronics Specialists Conf.*, pp. 925-931, June 2008.

[3] P.D. Mitcheson, E.M. Yeatman, G.K. Rao, A.S. Holmes, and T.C.Green, "Energy harvesting from human and machine motion for wireless electronic devices," *Proceedings of the IEEE*, vol. 96, no. 9, pp. 1457-1486, Sept. 2008.

[4] S. Roundy, P.K. Wright, and J.M. Rabaey, *Energy Scavenging for Wireless Sensor Networks with Special Focus on Vibrations*, 1st ed., Massachusetts: Kluwer Academic Publishers, 2004.

[5] H. Lhermet, C. Condemine, M. Plissonnier, R. Salot, P. Audebert, and M. Rosset, "Efficient power management circuit: from thermal energy harvesting to above-IC microbattery energy storage," *IEEE J. Solid-State Circuits*, vol. 43, no. 1, pp. 246-255, Jan. 2008.

[6] G.K. Ottman, H.F. Hofmann, A.C. Bhatt, and G.A. Lesieutre, "Adaptive piezoelectric energy harvesting circuit for wireless remote power supply," *IEEE Transactions on Power Electronics*, vol. 17, no. 5, pp. 669-676, Sept. 2002.

[7] D. Kwon and G.A. Rincón-Mora, "A rectifier-free piezoelectric energy harvester circuit," *Proc. IEEE International Symposium on Circuits and Systems (ISCAS)*, pp. 1085-1088, May 2009.

[8] Y. Lam, W. Ki, and C. Tsui, "Integrated low-loss CMOS active rectifier for wirelessly powered devices," *IEEE Transactions on Circuits and Systems II, Express Briefs*, vol. 53, no. 12, pp.1378-1382, Dec. 2006.

[9] T. Le, J. Han, A. von Jouanne, K. Mayaram, and T.S. Fiez, "Piezoelectric micro-power generation interface circuits," *IEEE J. Solid-State Circuits*, vol. 41, no. 6, pp. 1411-1420, June 2006.

[10] N.J. Guilar, R. Amirtharajah, and P.J. Hurst, "A full-wave rectifier with integrated peak selection for multiple electrode piezoelectric energy harvesters," *IEEE J. Solid-State Circuits*, vol. 44, no.1, pp. 240-246, Jan. 2009.

[11] Y.K. Ramadass and A.P. Chandrakasan, "An efficient piezoelectric energy-harvesting interface circuit using a bias-flip rectifier and shared inductor," *ISSCC Dig. Tech. Papers*, pp. 296-297, Feb. 2009.

[12] A. Badel, D. Guyomar, E. Lefeuvre, and C. Richard, "Piezoelectric energy harvesting using a synchronized switch technique," *J. Intelligent Material Systems and Structures*, vol. 17, pp. 831-839, Aug./Sept. 2006.

[13] D. Kwon and G.A. Rincón-Mora, "A single-inductor ac-dc piezoelectric energy-harvester/battery-charger IC converting ±(0.35 to 1.2V) to (2.7 to 4.5V)," *ISSCC Dig. Tech. Papers*, Feb. 2010.

[14] S. Meninger, J. Mur-Miranda, R. Amirtharajah, A. Chandrakasan, and J Lang, "Vibration-to-electric energy conversion," *IEEE Transactions on Very Large Scale Integration (VLSI) Systems*, vol. 9, no. 1, pp. 64-76, Feb. 2001.

[15] E.O. Torres and G.A. Rincón-Mora, "Electrostatic energy-harvesting and battery-charging CMOS system prototype," *IEEE Transactions on Circuits and Systems I*, vol. 56, no. 9, pp. 1938-1948, Sept. 2009.

[16] E.O. Torres and G.A. Rincón-Mora, "Energy budget and high-gain strategies for voltage-constrained electrostatic harvesters," *Proc. IEEE*

International Symposium on Circuits and Systems (ISCAS), pp. 1101-1104, May 2009.